Characterization of Cylinder-Forming Block Copolymers Directed to Assemble on Spotted Chemical Patterns

Sang-Min Park,[†] Gordon S. W. Craig,[†] Chi-Chun Liu,[†] Young-Hye La,[†] Nicola J. Ferrier,[‡] and Paul F. Nealey*[,†]

Department of Chemical and Biological Engineering and Department of Mechanical Engineering, University of Wisconsin—Madison, Madison, Wisconsin 53706

Received May 1, 2008; Revised Manuscript Received October 7, 2008

ABSTRACT: Films of cylinder-forming polystyrene-*block*-poly(methyl methacrylate) (bulk intercylinder spacing a_o) were directed to assemble on surfaces chemically patterned with a hexagonal array of spots (interspot spacing a_s). The block copolymer domain assembly was investigated as a function of the film thickness and the commensurability between a_o and a_s. The domains assembled vertically away from and matched the spacing and hexagonal order of the underlying lithographically patterned chemical substrate, provided a_s was equal to or up to 6% larger than a_o and the film thickness was ≤54 nm. In contrast, comparably poor assembly was obtained when a_s was 8% less than a_o. When a_s was commensurate with a_o, the cylinder diameter and eccentricity had a lower standard deviation and was more circular, respectively, than that of self-assembled cylinders on a neutral substrate.

Introduction

The self-assembly and perpendicular orientation of cylindrical block copolymer domains in thin films can be used to fabricate dense, periodic arrays of spot patterns with nanometer length scale.[1,2] Porous, thin (≤50 nm thick) films of block copolymer formed by the removal of the polymer in the cylindrical domains have been employed as a template for a host of applications, including the fabrication of MOSFET's,[3] quantum dots,[1,4,5] high surface area capacitors,[6] porous membranes,[7,8] and bit patterned media.[9] The dimensions of the block copolymer cylindrical domains can be determined via control of copolymer chain length,[10] addition of homopolymer,[11] and cross-linking during polymerization,[12] which has enhanced the interest in these materials.[1,2,10−14] Registration of the cylinders with respect to the underlying substrate and control of the order[15,16] of the hexagonal array of the cylinders are technologically significant objectives because they offer the potential to enable a broader range of applications, such as magnetic storage media[17] and integration in advanced lithography.[13,18−22]

A variety of methods have been developed to promote the vertical orientation of the cylindrical domains and to control the ordering of the hexagonal array of vertical cylinders. Vertically oriented domains have been achieved with chemically neutral surfaces,[23−26] electric fields,[27,28] addition of homopolymer,[29] control of solvent evaporation,[30] and solvent annealing.[31] Solvent annealing can also provide morphologies with very large grains of ordered domains.[32−34] In addition to cylinder orientation and ordering, for many applications, it is necessary for the domains to be aligned with underlying features on the substrate.[13,35] Topographically directed assembly[9,36−39] and chemical pattern directed assembly on square arrays[40] of cylinder-forming block copolymers are examples of methods to provide registration to the underlying substrate.

We investigate the use of surfaces that have been chemically nanopatterned with a hexagonal array of spots to direct the assembly of cylinder-forming block copolymers into arrays of perpendicular, hexagonally ordered cylinders. In a separate publication we have shown that we were able to achieve pattern density multiplication with an optimal film thickness of cylinder-forming block copolymer on a pattern that was commensurate with the domain spacing of the block copolymer.[41] Our work here is of fundamental importance because we delineate the degree of commensurability and thickness over which uniform, vertically oriented cylinders can be assembled on a chemical pattern as well as the factors that lead to the formation of more complicated three-dimensional (3D) structures. Such vertically oriented cylinders are of technological importance with respect to creating templates of different spacing, size, and aspect ratio. Previously, lamellae-forming block copolymers have been directed to assemble on striped chemical patterns.[42−44] We have investigated the control of domain dimensions, period, and shape as a function of the pattern surface energy,[42,45] size,[45−47] and geometry.[21,48] Similar to the previous work with chemically patterned surfaces, in the work presented here the interfacial energy contrast between the spots and matrix of the chemically patterned surface with the different blocks of the block copolymer creates a thermodynamic driving force that induces the orientation and ordering of the cylindrical domains as the copolymer film equilibrates in the presence of the chemically patterned surface. We quantify the diameter, uniformity, and eccentricity of the resulting cylinders as a function of film thickness and the commensurability between the chemical pattern spacing (a_s) and the bulk spacing between cylinders of the block copolymer (a_o).

Experimental Section

Materials. Asymmetric polystyrene-*block*-poly(methyl methacrylate) (P(S-*b*-MMA)) was purchased from Polymer Source, Inc., and used without purification. The number-average molecular weight, M_n, was 50.5 and 20.9 kg/mol for the PS and the PMMA blocks, respectively, and the resulting morphology consists of cylindrical PMMA domains surrounded by a PS matrix. χN, the product of the Flory−Huggins interaction parameter (χ) and the degree of polymerization (N), for the P(S-*b*-MMA) at the annealing temperature used in this study was calculated from values in the literature to be 25.2. a_o of the P(S-*b*-MMA) used in this work was 43.5 nm, and the mean diameter of the cylinder phase was 19.5 nm. Hydroxy-terminated polystyrene (PS-OH, M_n = 9.5 kg/mol) was purchased from Polymer Source, Inc. Nitroxide-mediated living free-radical polymerization was performed to synthesize a hydroxyl-

* To whom correspondence should be addressed: e-mail nealey@engr.wisc.edu; Tel 608-265-8171; Fax 608-262-5434.
[†] Department of Chemical and Biological Engineering.
[‡] Department of Mechanical Engineering.

10.1021/ma8009917 CCC: $40.75
Published on Web 11/04/2008

terminated random copolymer of styrene and methyl methacrylate (P(S-*r*-MMA)) with 58 vol % styrene. The PMMA resist used for electron beam patterning had a $M_n = 950$ kg/mol and was purchased from Microchem Corp.

Sample Preparation. The chemical patterns were fabricated with a method similar to previous work.[40] A thin layer of PS-OH was spin-coated onto a piranha-treated silicon wafer from a 1.5 wt % toluene solution and then heated under vacuum at 160 °C for 48 h to graft the PS-OH to the silicon substrates to form a PS brush. Ungrafted PS-OH was extracted by repeated rinses with warm toluene. The resulting thickness of the PS brush layer was about 7 nm. A 60 nm thick film of photoresist was spin-coated on the PS brush and baked at 160 °C for 60 s. Electron beam lithography was used to pattern hexagonal arrays of spots onto the photoresist. The electron beam lithography was performed with a LEO 1550-VP field emission scanning electron microscope (SEM) operating with a J.C. Nabity pattern generation system. The exposure used an accelerating voltage of 20 kV, a beam current of ~9 pA, and line doses centered at ~0.4 nC/cm. Development of samples was carried out by immersing them in a 1:3 mixture of methyl isobutyl ketone and isopropyl alcohol for 30 s, followed by rinsing with isopropyl alcohol and drying. After developing the sample, the hexagonal spot patterns were transferred into a chemical surface pattern in the PS brush layer via a brief oxygen plasma. Chemically nanopatterned substrates were spin-coated with a thin (30, 54, or 70 nm) film of cylinder-forming P(S-*b*-MMA) diblock copolymer and then annealed under vacuum at 180 °C for 48 h to form the equilibrium morphology. 30 nm thick films of P(S-*b*-MMA) were also coated on a chemically neutral[45,49,50] substrate made by grafting hydroxyl-terminated P(S-*r*-MMA) on a silicon wafer, as previously described in the literature.[48]

Analysis. The initial film thickness was measured by ellipsometry (Rudolph Research AutoEL-II). The block copolymer morphologies were imaged without a metal coating using a SEM with a 1 kV acceleration voltage. In order to improve the contrast in the SEM images, the PMMA block was selectively removed from the block copolymer film by UV irradiation (1 mJ/cm^2) followed by developing in 97% acetic acid. Quantitative information about the domain spacing of the P(S-*b*-MMA) on chemically neutral substrates was gathered from an analysis of the power spectra of two-dimensional fast Fourier transforms (2D-FFT) of SEM images. The intensities of the FFT power spectra were averaged azimuthally to yield the average intensity of the FFT in q-space ($q = 2\pi/L$). The first order peaks in these spectra were used to analyze the P(S-*b*-MMA) block copolymer domain periods on chemically neutral substrates. The domain spacings for the cylinders on the chemically patterned substrate were calculated from the positions of the cylinder centers, which were determined from image analysis of the SEMs. The coordinates of the center of each cylinder in the SEM image were determined by a least-squares fit of a Gaussian surface to the normalized grayscale level of the pixels in the SEM that comprise the given cylinder. The coordinates of each cylinder in a 2.8 μm by 3.8 μm area of a SEM image were then combined to generate an overlay plot of the 30 nearest neighbors to each cylinder. In the overlay plot, each central cylinder was located at the origin of coordinates, and the same orientation of axes was used for all of the central cylinders.

Results

We used spotted chemical surface patterns with a_s values of 40, 43, or 46 nm and the directed assembly process diagrammed in Figure 1 to investigate the effect of film thickness (t) and the commensurability between a_s and a_o on the assembly of cylindrical domains in thin films of P(S-*b*-MMA). Plan-view SEM was used to image the domains at the free surface of the equilibrated films. In the Discussion section we use our knowledge from previous work with directed assembly on chemical nanopatterns[45,51−53] to draw general conclusions about the likely 3D structure of the domains within the film.

The ability of the spotted chemical pattern to induce the formation of well-ordered arrays of domains as visualized at the free surface of the film depended on both a_s and film thickness t, as seen in the plan-view SEM images of P(S-*b*-MMA) films shown in Figure 2. The best hexagonal order in the SEM images was achieved with the 54 nm thick films in the case when a_s and a_o were approximately commensurate ($a_s = 43$ nm, $a_o = 43.5$ nm) or when a_s was 6% larger than a_o ($a_s = 46$ nm). When a_s was 8% less than a_o ($a_s = 40$), arrays of domains were observed at the free surface, but the hexagonal order of those domains had numerous defects. In the case of the 30 nm thick films, hexagonal order was again achieved when $a_s = 43$ or 46 nm. Some defects were apparent in the $a_s = 43$ nm sample, and more were apparent when $a_s = 40$ nm. In the thickest films ($t = 70$ nm), regardless of whether or not a_s and a_o were commensurate, P(S-*b*-MMA) assembled with some linear segments in the SEM images, indicative of PMMA domains parallel to the surface. Although we do not know the exact 3D structure of these domains parallel to the surface, we expect that they were half-cylinders and will refer to them as such. Despite the presence of these half-cylinders at the free surface in the 70 nm thick films, when a_s was 43 or 46 nm, the domains that appeared as circles in the SEM images still possessed a hexagonal arrangement.

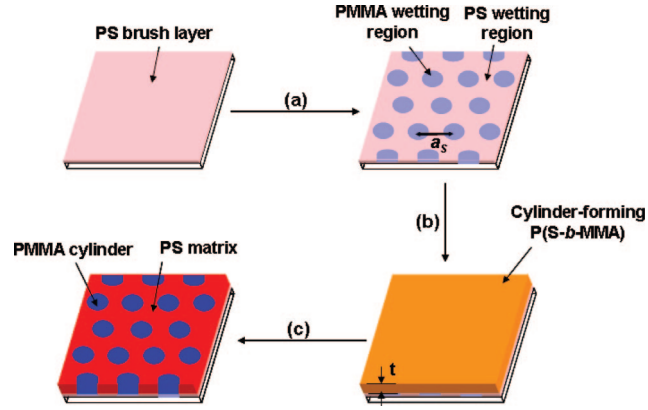

Figure 1. Schematic of procedure used to direct the assembly of cylinder-forming diblock copolymer on a chemical pattern consisting of a hexagonal array of spots. (a) The chemically patterned surface was produced in a PS brush layer using electron beam patterning and oxygen plasma treatment. (b) The chemically patterned surface was spin-coated with cylinder-forming diblock copolymer thin film. (c) The sample was annealed to achieve the equilibrium morphology.

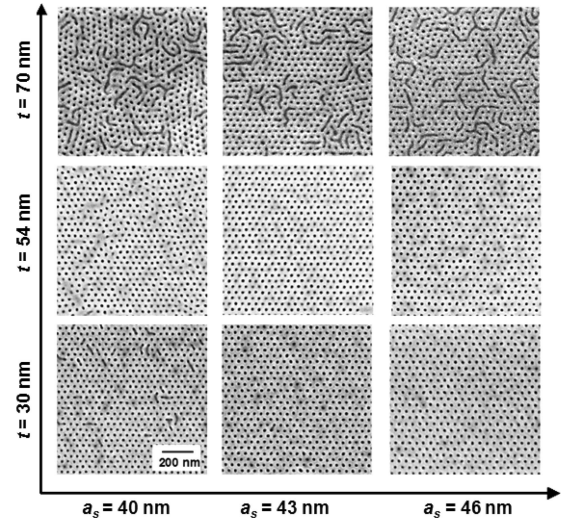

Figure 2. Top-down SEM images of 30, 54, and 70 nm thick films of P(S-*b*-MMA) directed to assemble on chemical patterns consisting of hexagonal arrays of spots with varying interspot distance (a_s).

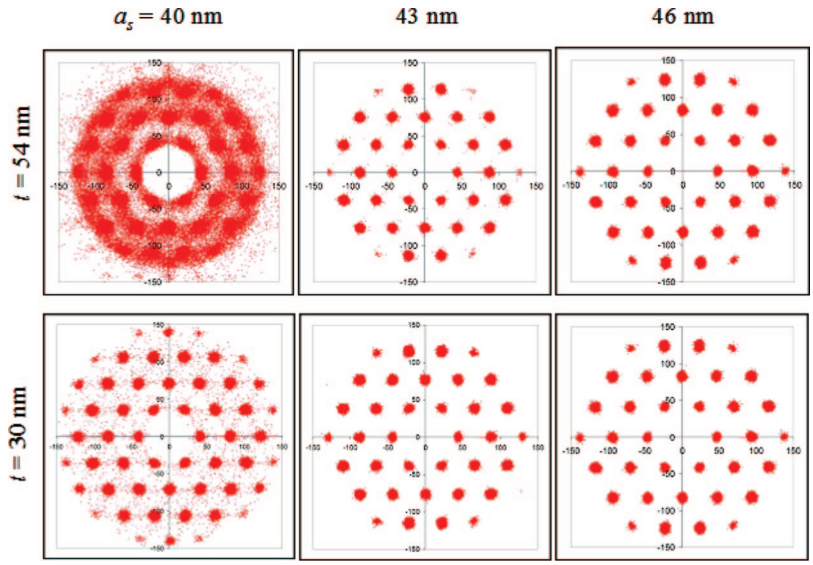

Figure 3. Superimposed plots of relative location of the 30 nearest neighbor cylinders around each cylinder after directed assembly of P(S-*b*-MMA) films of different thickness with varying a_s. The superimposed plot of the 54 nm thick sample with $a_s = 40$ nm resulted in 36 broad clusters due primarily to defects in the hexagonal order of the domains in the sample. Small clusters beyond the 30 nearest neighbors in the other five plots were caused primarily by the inclusion in the analysis of cylinders at the edge of the image.

The effect of t and a_s on the order could be seen more readily in the overlay plots of the position of the cylinder centers shown in Figure 3, which were generated as described in the Experimental Section from positional data determined from the plan-view SEM's shown in Figure 2. The most striking overlay plot was that of the film with $a_s = 40$ nm and $t = 54$ nm. The clusters of red dots in the overlay plot for this sample were so broad that they nearly formed a continuous ring. In contrast, the overlay plot at the same a_s value but at $t = 30$ had much tighter clusters of red dots, with some individual, scattered spots. Thus, as t increased from 30 to 54 nm, there was a significant decrease in the hexagonal order of the domains at the free surface of the film. Similarly, when a_s was decreased from 43 to 40 nm in the 54 nm thick films, there was a significant decrease in the order of the film, as seen in a comparison of the corresponding overlay plots. In contrast, when a_s was increased from 43 to 46 nm, tight clusters of spots were obtained in the overlay plots for both the 30 and 54 nm thick films.

In order to investigate the cylinder array in detail, a quantitative analysis of the dimensions and positional order of the cylindrical domains at the free surface of the P(S-*b*-MMA) thin films was carried out using the cylinder positional data overlaid in Figure 3. Figure 4 shows average values of the intercylinder distance a at the free surface of the six nearest neighbors in the assembled block copolymer thin films. In the 30 nm thick films, a equaled a_s for all of the samples. In the 54 nm thick films, $a = a_s$ when a_s was 43 or 46 nm, but $a = a_o$ when $a_s = 40$ nm. Thus, when the hexagonal order of the films was good, the spacing of the domains at the free surface of the film matched the chemical pattern spacing, but when the hexagonal order was poor, as in the case of the 54 nm thick film with $a_s = 40$ nm, the spacing of the domains was the same as in the bulk polymer.

We also measured the mean diameter, d, and eccentricity, ε, of the cylinder domains at the free surface of the film ($\varepsilon^2 = 1 - m^2/l^2$, where l and m are the major and minor axes of the cylinder cross section, respectively) and then plotted the results as shown in Figure 5. The average cylinder diameter of P(S-*b*-MMA) in 30 nm thick films depended on a_s. When 30 nm thick films of P(S-*b*-MMA) were directed to assemble on a chemical pattern with $a_s = 40$ nm, d was 17 nm, whereas it increased to 20 nm on chemical patterns with $a_s = 46$ nm. The

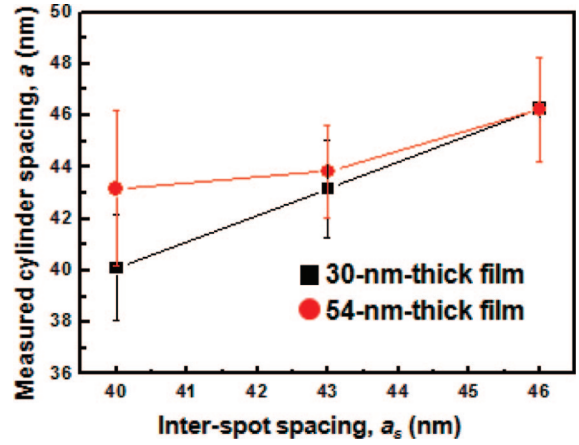

Figure 4. Plot of intercylinder distance (a) of thin films of P(S-*b*-MMA) directed to assemble on chemically spot-patterned surfaces with varying interspot distance (a_s). The error bars shown denote the standard deviation of the measured distance at each a_s value.

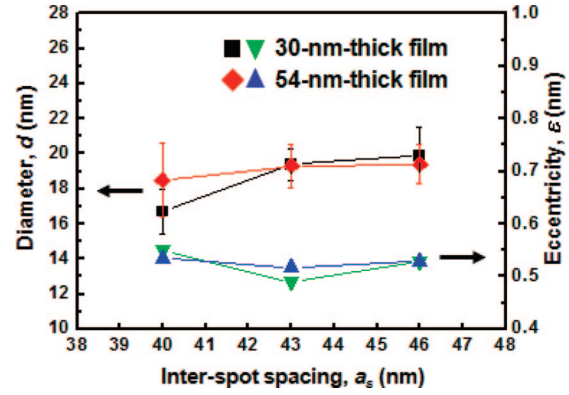

Figure 5. Diameter (d) and eccentricity (ε) of cylindrical structures directed to assemble on chemically spot-patterned surfaces with varying interspot distance (a_s). The error bars shown denote the standard deviation of the measured diameter at each a_s value.

diameter of the cylinder on the $a_s = 43$ nm pattern was 19.4 nm, almost the same as the size of cylindrical domains in the bulk. Also, the cylinders on the $a_s = 43$ nm pattern achieved a

very narrow size distribution, with a ratio of the standard deviation to the mean diameter (σ/d) of 0.046.

Discussion

Previous studies on directed assembly have shown that, within limits of thickness and pattern/copolymer commensurability, the interfacial energy between the block copolymer and the chemical pattern can be large enough to change the dimensions or geometry of the morphology in a thin film of block copolymer as it equilibrates in the presence of the chemical pattern, but beyond those limits of commensurability or thickness, 3D structures form in the film. For example, when lamellae-forming P(S-*b*-MMA) was assembled on striped patterns formed in PS-OH brushes like the brushes used in this study, the interfacial energy was sufficient to cause the lamellar period of the assembled copolymer, L, to equal the period of the chemical pattern, L_s, even when L_s was 10% larger or smaller than the bulk lamellar period, L_o.[45] Indeed, the interfacial energy supplied to a thin film of block copolymer can have an impact large enough to convert a hexagonal array of cylindrical domains into a square array.[40] What drives the assembly of the domains into spacings or geometries that are different from the bulk is the interfacial energy between the chemical pattern and the block copolymer, which results in a strongly preferential wetting of the PMMA and PS blocks to the oxidized and unoxidized regions of the pattern, respectively.[54] However, when the limits of pattern commensurability or thickness are exceeded, 3D structures will form,[55] and in the case of cylindrical domains, these 3D structures can take the form of semicylinders or loop structures.[40] On the basis of our knowledge from these previous experimental studies, as well as previous simulations of cylindrical domains on chemically patterned substrates,[56] we can conclude that if the domains at the free surface were ordered, then they extended through the film as vertical cylinders with $a = a_s$, but if the domains were not ordered, a 3D structure existed within the film, and the spacing of the cylinders were approximately a_o.

Applying this insight into the images in Figure 2, we conclude that well-ordered, perpendicular cylinders were formed in the 30 and 54 nm thick films with a_s equal to 43 or 46 nm. It is technologically significant that we were able to achieve ordered, perpendicular cylinders in 54 nm thick films, which was significantly thicker than the 40 nm thickness that Guarini et al. found to be optimal for forming, on a neutral substrate, ordered cylinders that were amenable for pattern transfer.[57] A 3D structure containing half-cylinders formed in all of the 70 nm thick films. A comparison of the 30 and 54 nm thick films with $a_s = 40$ nm reveals two different types of defects. The decrease in order of the 54 nm thick film when $a_s = 40$ nm indicated that a 3D structure, perhaps consisting of tortuous or bent cylinders, had formed in this sample. Additionally, $a = a_o$ for the 54 nm thick film on the pattern with $a_s = 40$ nm, suggesting that the 3D structure had developed in the film to convert the cylinder spacing from a_s at the interface to the value of a_o plotted in Figure 4. By contrast, $a = a_s$ in the 30 nm thick film with $a_s = 40$ nm, such that even though some defects were apparent in the sample, the underlying chemical pattern was still effective in directing the assembly of the domains. The overlay plot in Figure 3 also shows that this sample had a high degree of order. Thus, the sample had a predominance of perpendicular cylinders through the thickness of the film, with a small percentage of defects that could have been loop cylinders, such as those observed previously.[40]

The diminishing ability of the chemical pattern to form perpendicular cylinders and ordered cylindrical domains as t increases can be seen in all of the samples on chemical patterns with $a_s = 40$ nm as well as in the contrast between the 54 and 70 nm thick films. Insight into the origin of this loss of guidance from the chemical pattern can be found from analysis of the free energy F of the block copolymer film on the chemical pattern, which can be expressed as the sum of free energy terms for the chain conformation ($F_{elastic}$), the domain−domain interface ($F_{S\text{-}MMA}$), the free surface ($F_{surface}$), and the chemical pattern−block copolymer interface ($F_{interface}$):[45]

$$F = F_{elastic} + F_{S\text{-}MMA} + F_{surface} + F_{interface} \quad (1)$$

In order for the chemical pattern to direct the cylindrical domains to orient perpendicularly throughout the film, the contribution of $F_{interface}$ must be such that F is minimized when the desired morphology is formed at equilibrium. If 3D structures are observed in the film, then either the desired morphology is no longer the structure that represents the minimization of F or the minima of F at the desired morphology is not deep enough to suppress the formation of low energy defects. We can focus on the $F_{interface}$ term in eq 1 by considering those samples for which $a_s \approx a_o$ ($a_s = 43$ nm) because $F_{elastic}$ and $F_{S\text{-}MMA}$ approximately offset each other at equilibrium at the bulk spacing of a_o. There still exist components of $F_{elastic}$ and $F_{S\text{-}MMA}$ due to hard surface effects, but these components are relatively weak and play a role only when other energetic factors are correspondingly small.[58] Also, for P(S-*b*-MMA) we can consider the contribution of $F_{surface}$ to be relatively small because the surface energy of PS and of PMMA with respect to air (γ_{PS} and γ_{PMMA}) are very similar at the annealing temperature of 180 °C (differing at most by a few percent, with γ_{PMMA} greater than γ_{PS}).[50,59] Regarding $F_{interface}$, in the most simple case, on a per chain basis $F_{interface}$ is proportional to $1/t$.[45] As a result, as t increases, the chemical pattern supplies less energy to the total system on a per chain basis, and other energetic factors can play a role. Clearly for the results here, when t increased from 54 to 70 nm, $F_{interface}$ no longer provided sufficient energy to direct the orientation of all of the domains throughout the thickness of the film, and low energy defects appeared, which took the form of half-cylinders parallel to the free surface.

There are a number of possible explanations for the half-cylinders observed at the free surface of the 70 nm thick films, which have been seen before in thin films of P(S-*b*-MMA).[60,61] The preference for chain ends to reside at the free surface of a block copolymer film would favor the formation of domains parallel to the surface in asymmetric block copolymers.[62,63] Also, cylindrical domains in thin films on chemically patterned[61] or PMMA-preferential[64] substrates prefer to be parallel to the substrate when t is approximately commensurate with the spacing between layers of cylinders in the films, L_c ($2L_c = 75.3$ nm here).[61,64] Additionally, it is possible that loop structures,[40] which could take the form of inverted "U"s in the film, could be present in the 70 nm thick films. Finally, as stated above, if the minimum of F is not sufficiently deep to suppress low energy defects, it is possible for the observed morphology to continue to change with continued annealing, with some defects disappearing and others appearing.

The asymmetry of order and perfection of the equilibrated structures about a_o, such as the differences between the samples with $a_s = 40$ or 46 nm in the 30 and 54 nm thick films, can also be interpreted within the framework of the free energy of the block copolymer film as it equilibrates on the chemical pattern, but in this case it is necessary to have a better understanding of the effect that the commensurability of a_s and a_o has on $F_{elastic}$ and $F_{S\text{-}MMA}$. Suh et al.[65] built on previous work[66,67] to develop an expression for $F_{elastic} + F_{S\text{-}MMA}$ for cylindrical domains in the strong segregation regime (SSR). Although the block copolymer used here had a χN of 25.2 and therefore was in the intermediate segregation regime (ISR),[68] Matsen et al. have shown that the phenomena used to describe

behavior in SSR can also explains behavior in the ISR.[69] Additionally, Matsen compared SSR to self-consistent field theory (SCFT) and found that SSR and SCFT produced very similar phase diagrams and that the phase behavior changed very little for $\chi N \geq 20$.[70] For these reasons we feel confident in applying the model of Suh et al., which gives $F_{elastic} + F_{S\text{-}MMA}$ as

$$F_{elastic} + F_{S\text{-}MMA} = 3.81\frac{N\gamma}{\rho s}\sqrt{\phi} + \frac{3}{2}k_B T\left[As^2 + \frac{B}{s^2} - 4\right] \quad (2)$$

where

$$s = \frac{R_{MMA}}{1-\sqrt{\phi}}\sqrt{\frac{2\pi}{\sqrt{3}}} = \frac{R_S}{\sqrt{\phi}}\sqrt{\frac{2\pi}{\sqrt{3}}} \quad (3)$$

$$A = \frac{\sqrt{3}}{2\pi R_{MMA,0}^2}\phi + \frac{\sqrt{3}}{2\pi R_{S,0}^2}(1-\sqrt{\phi})^2 \quad (4)$$

and

$$B = \frac{2\pi R_{MMA,0}^2}{\sqrt{3}\phi} + \frac{2\pi R_{S,0}^2}{\sqrt{3}(1-\sqrt{\phi})^2} \quad (5)$$

For eqs 2−5, N is the degree of polymerization, γ is the domain interfacial tension, ρ is the repeat unit density, ϕ is the volume fraction of PMMA, p is the number of copolymer chains in the system, and $R_{MMA,0}$ and $R_{S,0}$ are the ideal Gaussian chain end-to-end distance of each block. R_{MMA} and R_S are the end-to-end distance of each block in the equilibrated block copolymer morphology and scale linearly with s as shown in eq 3. In the Alexander−de Gennes formalism the end-to-end distance is taken as the thickness of the layer in the structure corresponding to each block,[66] such that s scales with a in our study. When the sum $F_{elastic} + F_{S\text{-}MMA}$ is plotted versus s, the resulting curve has a minimum at s_o, which corresponds to a_o in our system, and the sum increases more rapidly as s moves away from s_o when $s < s_o$ than when $s > s_o$.[65]

Applied to our work here, on a per chain basis $F_{elastic} + F_{S\text{-}MMA}$ increases more rapidly as a moves away from a_o when $a < a_o$ than when $a > a_o$. Assuming that $F_{interface}$ is sufficient to direct the assembly of the domains when $a_s = a_o$, to direct the assembly of the block copolymer domains when $a_s \neq a_o$, $F_{interface}$ must overcome the increase in $F_{elastic} + F_{S\text{-}MMA}$ from its minimum at a_o to its value at a_s, which we denote as $\Delta F_{elastic} + \Delta F_{S\text{-}MMA}$. Taking into account the asymmetry of $F_{elastic} + F_{S\text{-}MMA}$ about a_o, the ability of the chemical pattern to induce a domain structure in which $a = a_s$ decreases more rapidly as a_s moves away from a_o when $a_s < a_o$ than when $a_s > a_o$. Applying this idea to either the 30 or 54 nm thick series of films, when a_s was 43 nm, $F_{elastic} + F_{S\text{-}MMA}$ was near its minimum at a_o, and $F_{interface}$ could easily dominate eq 1. When a_s was 46 nm (6% greater than a_o), the resulting well-ordered structures with $a = a_s$ observed at the free surface of the film again suggest that $F_{interface}$ was still able to overcome $\Delta F_{elastic} + \Delta F_{S\text{-}MMA}$. But, as outlined above, when $a_s = 40$ nm (8% less than a_o) structures either had more defects ($t = 30$ nm) or had $a = a_o$ ($t = 54$ nm). Although there was a difference in the magnitude of the incommensurability of the $a_s = 40$ nm and $a_s = 46$ nm films (6% vs 8%), it is likely that the primary cause of the asymmetry of the order and perfection of the equilibrated structures about a_o was due to the asymmetry in $F_{elastic} + F_{S\text{-}MMA}$ with respect to a. Because of this asymmetry in $F_{elastic} + F_{S\text{-}MMA}$, the block copolymer could more readily equilibrate in an expanded configuration than in a compressed configuration. Similar asymmetry has been observed in the topographically directed assembly of spherical microdomains,[71] but not in the directed assembly of lamellar domains.[45]

The change in the structure of the 30 and 54 nm thick films with $a_s = 40$ nm, going from ordered, perpendicular domains with a few defects and $a = a_s$ at $t = 30$ nm to a disordered structure with $a = a_o$ at $t = 54$ nm, can be understood when both the effect of thickness on $F_{interface}$ per chain and the asymmetry of $F_{elastic} + F_S$ about a_o are taken into account. For the films with $a_s = 40$, on a per chain basis $F_{interface}$ was still sufficiently large at $t = 30$ nm to overcome $\Delta F_{elastic} + \Delta F_{S\text{-}MMA}$, such that the interface could induce a structure with $a = a_s$. But due to the decrease of $F_{interface}$ per chain with t, when $t = 54$ nm $F_{interface}$ could not overcome $\Delta F_{elastic} + \Delta F_{S\text{-}MMA}$ when $a_s = 40$, and the minimization of F in eq 1 resulted in $a = a_o$.

In analyzing the effect that a_s and t had on the shape and dimensions of the individual cylinders, the role of t and the commensurability of a_s and a_o can be observed. When a_s and a_o were commensurate, the lowest σ/d (0.46) was achieved (Figure 5), which was significantly less than the 0.10 value reported for the self-assembly of P(S-*b*-MMA) cylinders on a neutral substrate,[8] but consistent with the range of 0.043−0.053 reported for topographically directed assembly of cylinders on a neutral substrate.[9] Similarly, the lowest ε value was achieved in the 30 nm thick film when a_s and a_o were commensurate. As t increased from 30 to 54 nm, both d and ε were relatively constant regardless of a_s and also close to the corresponding dimensions of the bulk copolymer. However, in the case of the σ/d value reported for cylinders on an unpatterned neutral substrate, it is possible that much of the increase in σ/d compared to the values reported here and on topographically patterned substrates was caused by the deformation of cylinders at grain boundaries in the hexagonal arrangement of the cylinders. Similarly, defects in hexagonal order would inherently lead to lower values of ε because there would be less deformation of individual domains. Thus, the best values that we observed in this study for both σ/d and ε could have been caused by the chemical pattern itself, by the improved order induced by the chemical pattern, or by both factors.

Conclusion

This work demonstrates that spotted chemical nanopatterns can direct the assembly of cylinder-forming block copolymers to form ordered arrays of perpendicular domains with a high degree of perfection. Such well-ordered domains could be achieved in films up to 54 nm thick when the spacing of the chemical pattern was commensurate with or up to 6% larger than the bulk copolymer domain spacing. The range of commensurability and film thickness over which one could expect to achieve well-ordered domain assembly can be understood in terms of the minimization of free energy as the block copolymer equilibrates in the present of a chemical pattern. Additionally, a high degree of cylinder uniformity was achieved over the same range of film thickness and commensurability parameters that yielded perpendicular arrays with a high degree of perfection. The ability to generate uniform, ordered, registered, hexagonal arrays of vertical cylinders could benefit a variety of technological applications of thin films of block copolymers, including template formation in advanced lithography. The improvement of the uniformity of the shape of the cylinders could find use in applications such as semiconductor manufacturing and magnetic storage media, where precision of critical dimensions is crucial.

Acknowledgment. This work was supported by the Semiconductor Research Corporation (SRC) (2005-MJ-985) and the National Science Foundation through the Nanoscale Science and Engineering Center (DMR-0425880). This work was based upon research conducted at the Synchrotron Radiation Center, University of Wisconsin−Madison, which is supported by the NSF under Award DMR-0537588.

References and Notes

(1) Shin, K.; Leach, K. A.; Goldbach, J. T.; Kim, D. H.; Jho, J. Y.; Tuominen, M.; Hawker, C. J.; Russell, T. P. *Nano Lett.* **2002**, *2*, 933.
(2) Thurn-Albrecht, T.; Steiner, R.; DeRouchey, J.; Stafford, C. M.; Huang, E.; Bal, M.; Tuominen, M.; Hawker, C. J.; Russell, T. P. *Adv. Mater.* **2000**, *12*, 1138.
(3) Chang, L.-W.; Wong, H.-S. P. *Proc. SPIE* **2006**, *2006*, 615611.
(4) Zhang, Q. L.; Xu, T.; Butterfield, D.; Misner, M. J.; Ryu, D. Y.; Emrick, T.; Russell, T. P. *Nano Lett.* **2005**, *5*, 357.
(5) Park, J. H.; Khandekar, A. A.; Park, S. M.; Mawst, L. J.; Kuech, T. F.; Nealey, P. F. *J. Cryst. Growth* **2006**, *297*, 283.
(6) Black, C. T.; Guarini, K. W.; Milkove, K. R.; Baker, S. M.; Russell, T. P.; Tuominen, M. T. *Appl. Phys. Lett.* **2001**, *79*, 409.
(7) Yang, S. Y.; Ryu, I.; Kim, H. Y.; Kim, J. K.; Jang, S. K.; Russell, T. P. *Adv. Mater.* **2006**, *18*, 709.
(8) Black, C. T.; Guarini, K. W.; Breyta, G.; Colburn, M. C.; Ruiz, R.; Sandstrom, R. L.; Sikorski, E. M.; Zhang, Y. *J. Vac. Sci. Technol., B* **2006**, *24*, 3188.
(9) Xiao, S. G.; Yang, X. M. *J. Vac. Sci. Technol., B* **2007**, *25*, 1953.
(10) Xu, T.; Kim, H. C.; DeRouchey, J.; Seney, C.; Levesque, C.; Martin, P.; Stafford, C. M.; Russell, T. P. *Polymer* **2001**, *42*, 9091.
(11) Jeong, U. Y.; Kim, H. C.; Rodriguez, R. L.; Tsai, I. Y.; Stafford, C. M.; Kim, J. K.; Hawker, C. J.; Russell, T. P. *Adv. Mater.* **2002**, *14*, 274.
(12) Jeong, U. Y.; Ryu, D. Y.; Kim, J. K.; Kim, D. H.; Russell, T. P.; Hawker, C. J. *Adv. Mater.* **2003**, *15*, 1247.
(13) Hawker, C. J.; Russell, T. P. *MRS Bull.* **2005**, *30*, 952.
(14) Segalman, R. A. *Mater. Sci. Eng., R* **2005**, *48*, 191.
(15) Puglisi, R. A.; Fata, P. L.; Lombardo, S. *Appl. Phys. Lett.* **2007**, *91*, 053104.
(16) Segalman, R. A.; Hexemer, A.; Hayward, R. C.; Kramer, E. J. *Macromolecules* **2003**, *36*, 3272.
(17) Service, R. F. *Science* **2006**, *314*, 1868.
(18) Black, C. T.; Ruiz, R.; Breyta, G.; Cheng, J. Y.; Colburn, M. E.; Guarini, K. W.; Kim, H. C.; Zhang, Y. *IBM J. Res. Dev.* **2007**, *51*, 605.
(19) Park, M.; Harrison, C.; Chaikin, P. M.; Register, R. A.; Adamson, D. H. *Science* **1997**, *276*, 1401.
(20) Stoykovich, M. P.; Kang, H.; Daoulas, K. C.; Liu, G.; Liu, C. C.; de Pablo, J. J.; Mueller, M.; Nealey, P. F. *ACS Nano* **2007**, *1*, 168.
(21) Stoykovich, M. P.; Muller, M.; Kim, S. O.; Solak, H. H.; Edwards, E. W.; de Pablo, J. J.; Nealey, P. F. *Science* **2005**, *308*, 1442.
(22) Stoykovich, M. P.; Nealey, P. F. *Mater. Today* **2006**, *9*, 20.
(23) Huang, E.; Rockford, L.; Russell, T. P.; Hawker, C. J. *Nature (London)* **1998**, *395*, 757.
(24) Ryu, D. Y.; Shin, K.; Drockenmuller, E.; Hawker, C. J.; Russell, T. P. *Science* **2005**, *308*, 236.
(25) Han, E.; In, I.; Park, S. M.; La, Y. H.; Wang, Y.; Nealey, P. F.; Gopalan, P. *Adv. Mater.* **2007**, *19*, 4448.
(26) Bang, J.; Kim, S. H.; Drockenmuller, E.; Misner, M. J.; Russell, T. P.; Hawker, C. J. *J. Am. Chem. Soc.* **2006**, *128*, 7622.
(27) Mansky, P.; DeRouchey, J.; Russell, T. P.; Mays, J.; Pitsikalis, M.; Morkved, T.; Jaeger, H. *Macromolecules* **1998**, *31*, 4399.
(28) Morkved, T. L.; Lu, M.; Urbas, A. M.; Ehrichs, E. E.; Jaeger, H. M.; Mansky, P.; Russell, T. P. *Science* **1996**, *273*, 931.
(29) Kitano, H.; Akasaka, S.; Inoue, T.; Chen, F.; Takenaka, M.; Hasegawa, H.; Yoshida, H.; Nagano, H. *Langmuir* **2007**, *23*, 6404.
(30) Kim, G.; Libera, M. *Macromolecules* **1998**, *31*, 2569.
(31) Sidorenko, A.; Tokarev, I.; Minko, S.; Stamm, M. *J. Am. Chem. Soc.* **2003**, *125*, 12211.
(32) Kim, S. H.; Misner, M. J.; Russell, T. P. *Adv. Mater.* **2004**, *16*, 2119.
(33) Kim, S. H.; Misner, M. J.; Xu, T.; Kimura, M.; Russell, T. P. *Adv. Mater.* **2004**, *16*, 226.
(34) Kim, S. H.; Misner, M. J.; Yang, L.; Gang, O.; Ocko, B. M.; Russell, T. P. *Macromolecules* **2006**, *39*, 8473.
(35) Cheng, J. Y.; Ross, C. A.; Smith, H. I.; Thomas, E. L. *Adv. Mater.* **2006**, *18*, 2505.
(36) Black, C. T.; Bezencenet, O. *IEEE Trans. Nanotechnol.* **2004**, *3*, 412.
(37) Cheng, J. Y.; Zhang, F.; Smith, H. I.; Vancso, G. J.; Ross, C. A. *Adv. Mater.* **2006**, *18*, 597.
(38) Sundrani, D.; Sibener, S. J. *Macromolecules* **2002**, *35*, 8531.
(39) Yang, X. M.; Xiao, S. G.; Liu, C.; Pelhos, K.; Minor, K. *J. Vac. Sci. Technol., B* **2004**, *22*, 3331.
(40) Park, S. M.; Craig, G. S. W.; La, Y. H.; Solak, H. H.; Nealey, P. F. *Macromolecules* **2007**, *40*, 5084.
(41) Ruiz, R.; Kang, H.; Detcheverry, F. A.; Dobisz, E.; Kercher, D. S.; Albrecht, T. R.; de Pablo, J. J.; Nealey, P. F. *Science* **2008**, *321*, 936.
(42) Kim, S. O.; Solak, H. H.; Stoykovich, M. P.; Ferrier, N. J.; de Pablo, J. J.; Nealey, P. F. *Nature (London)* **2003**, *424*, 411.
(43) Peters, R. D.; Yang, X. M.; Wang, Q.; de Pablo, J. J.; Nealey, P. F. *J. Vac. Sci. Technol., B* **2000**, *18*, 3530.
(44) Rockford, L.; Liu, Y.; Mansky, P.; Russell, T. P.; Yoon, M.; Mochrie, S. G. J. *Phys. Rev. Lett.* **1999**, *82*, 2602.
(45) Edwards, E. W.; Montague, M. F.; Solak, H. H.; Hawker, C. J.; Nealey, P. F. *Adv. Mater.* **2004**, *16*, 1315.
(46) Kim, S. O.; Kim, B. H.; Kim, K.; Koo, C. M.; Stoykovich, M. P.; Nealey, P. F.; Solak, H. H. *Macromolecules* **2006**, *39*, 5466.
(47) Edwards, E. W.; Muller, M.; Stoykovich, M. P.; Solak, H. H.; de Pablo, J. J.; Nealey, P. F. *Macromolecules* **2007**, *40*, 90.
(48) Park, S. M.; La, Y. H.; Ravindran, P.; Craig, G. S. W.; Ferrier, N. J.; Nealey, P. F. *Langmuir* **2007**, *23*, 9037.
(49) In, I.; La, Y. H.; Park, S. M.; Nealey, P. F.; Gopalan, P. *Langmuir* **2006**, *22*, 7855.
(50) Mansky, P.; Liu, Y.; Huang, E.; Russell, T. P.; Hawker, C. *Science* **1997**, *275*, 1458.
(51) Craig, G. S. W.; Nealey, P. F. *J. Vac. Sci. Technol., B* **2007**, *25*, 1969.
(52) Nealey, P. F.; Edwards, E. W.; Müller, M.; Stoykovich, M. P.; Solak, H. H.; De Pablo, J. J. *IEEE Tech. Dig. IEDM* **2005**, 356.
(53) Stoykovich, M. P.; Edwards, E. W.; Solak, H. H.; Nealey, P. F. *Phys. Rev. Lett.* **2006**, *97*000.
(54) Edwards, E. W.; Stoykovich, M. P.; Muller, M.; Solak, H. H.; De Pablo, J. J.; Nealey, P. F. *J. Polym. Sci., Part B: Polym. Phys.* **2005**, *43*, 3444.
(55) Daoulas, K. C.; Muller, M.; Stoykovich, M. P.; Park, S. M.; Papakonstantopoulos, Y. J.; de Pablo, J. J.; Nealey, P. F.; Solak, H. H. *Phys. Rev. Lett.* **2006**, *96*000.
(56) Wang, Q.; Nealey, P. F.; de Pablo, J. J. *Macromolecules* **2003**, *36*, 1731.
(57) Guarini, K. W.; Black, C. T.; Yeuing, S. H. I. *Adv. Mater.* **2002**, *14*, 1290.
(58) Meng, D.; Wang, Q. *J. Chem. Phys.* **2007**, *126*000.
(59) Mansky, P.; Russell, T. P.; Hawker, C. J.; Mays, J.; Cook, D. C.; Satija, S. K. *Phys. Rev. Lett.* **1997**, *79*, 237.
(60) Ruiz, R.; Sandstrom, R. L.; Black, C. T. *Adv. Mater.* **2007**, *19*, 587.
(61) Edwards, E. W.; Stoykovich, M. P.; Solak, H. H.; Nealey, P. F. *Macromolecules* **2006**, *39*, 3598.
(62) Wang, J. S.; Binder, K. *J. Phys. I* **1991**, *1*, 1583.
(63) Wang, Q.; Nealey, P. F.; de Pablo, J. J. *Macromolecules* **2001**, *34*, 3458.
(64) Yang, Y. Z.; Qiu, F.; Zhang, H. D.; Yang, Y. L. *Polymer* **2006**, *47*, 2205.
(65) Suh, K. Y.; Kim, Y. S.; Lee, H. H. *J. Chem. Phys.* **1998**, *108*, 1253.
(66) Gido, S. P.; Schwark, D. W.; Thomas, E. L.; do Carmo Goncalves, M. *Macromolecules* **1993**, *26*, 2636.
(67) Leibler, L.; Orland, H.; Wheeler, J. C. *J. Chem. Phys.* **1983**, *79*, 3550.
(68) Leibler, L. *Macromolecules* **1980**, *13*, 1602.
(69) Matsen, M. W.; Bates, F. S. *J. Chem. Phys.* **1997**, *106*, 2436.
(70) Matsen, M. W. *J. Chem. Phys.* **1997**, *106*, 7781.
(71) Cheng, J. Y.; Mayes, A. M.; Ross, C. A. *Nat. Mater.* **2004**, *3*, 823.

MA8009917